Power and Energy Management with Battery Storage for a Hybrid Residential PV-Wind System

A Case Study for Denmark

Stroe, Daniel-Ioan; Zaharof, Andreea; Iov, Florin

Published in:
Energy Procedia

DOI (link to publication from Publisher):
10.1016/j.egypro.2018.11.033

Publication date:
2018

Document Version
Publisher's PDF, also known as Version of record

Available online at www.sciencedirect.com

ScienceDirect

Energy Procedia 155 (2018) 464–477

Energy Procedia

www.elsevier.com/locate/procedia

12th International Renewable Energy Storage Conference, IRES 2018

Power and Energy Management with Battery Storage for a Hybrid Residential PV-Wind System – A Case Study for Denmark

Daniel-Ioan Stroe[a]*, Andreea Zaharof[a], Florin Iov[a]

[a]*Department of Energy Technology, Aalborg University, 9220 Aalbor Øst, Denmark*

Abstract

The energy generation paradigm is shifting from centralized fossil-fuel-based generation to distributed-based renewable generation. Thus, hybrid residential energy systems based on wind turbines, PV panels and/or micro-turbines are gaining more and more terrain. Nevertheless, such a system needs to be coupled with an energy storage solution, most often a battery, in order to mitigate its power generation variability and to ensure a stable and reliable operation. In this work, two power and energy management strategies for a hybrid residential PV-wind system with battery energy storage were evaluated. Simple but customized performance models for PV modules and a small wind turbine have been developed; furthermore, the models have been parameterized based on real-life time-series for irradiance and wind speed, characteristic for a site in Denmark. The stress, to which the battery was subjected, while providing the two energy management strategies, was also quantified.

Keywords: Battery, Residential PV-Wind System, Power, Energy

1. Introduction

The solar photovoltaic (PV) total installed capacity in Denmark has exponentially increased in the last years. According to the International Renewable Energy Agency, the cumulative solar PV capacity increased from 17 MW

* Corresponding author. Tel.: +45-3062 2589; fax: +45-9940 3820.
E-mail address: dis@et.aau.dk

10.1016/j.egypro.2018.11.033

in 2011 to 399 MW in 2012, reaching 790.4 MW by the end of 2016 [1]. The vast majority of the installations (approx. 95%) are represented by residential roof-top PV systems with power levels below 6 kW. This trend is expected to continue as by 2020 the aim is to generate 5% of electricity from residential solar PV systems [2]. Furthermore, Denmark has always been a leader in the wind power production sector. Nowadays, approximately 33% of the installed wind turbines have a rated power below 25 kW and most of the times they are connected to the low voltage grid [3]. These renewables' grid integration trends combined with the presence of new loads such as heat pumps and electric vehicles are threatening the stable and reliable operation of low voltage grids causing voltage unbalances, neutral point displacement, voltage flickers etc.

The aforementioned issues can be mitigated using battery energy storage [4], [5]. Among the available storage technologies, Lithium-ion batteries represent an obvious solution because of their characteristics (e.g., high efficiency, long lifetime, low self-discharge) combined with rapid price decrease [5], [6]. Nevertheless, the installations of such systems should be accompanied by the availability of a power and energy management system, which will control and optimize the power flow by providing different services to the grid and/ or to the end-user (e.g., power smoothing, peak shaving, self-consumption maximization etc.) [7].

The aim of this paper is to investigate different power and energy management strategies for a hybrid residential PV-wind system using a Lithium-ion battery energy storage. It is well known that the performance of Lithium-ion batteries is very sensitive to the operating conditions (i.e., load current, temperature, state-of-charge, state-of-health). Thus, in order to develop accurate power and energy management strategies, a Lithium-ion battery electric model was developed and parameterized based on extensive laboratory tests. Furthermore, we have developed simple and robust performance models for a small wind turbine and solar PV panels. In our work we have investigated two power and energy management strategies for our hybrid energy system: power smoothing (using a moving average filter for 5 and 15 minutes) and energy blocks (i.e., constant power to/from the grid during 15 minutes). In order to perform realistic study cases, we have used real-life data for PV generation, wind power generation, and residential household consumption with a one-second resolution.

2. System Description and Modeling

The overview configuration of the considered hybrid residential PV-wind system with loads and battery storage is presented in Fig. 1. The system is composed of 17 PV modules with a power of 360 W each (i.e., approx. 6 kW system), a 10 kW small wind turbine, the household's loads and a Li-ion battery storage system. The smart meter between the household side and the utility side enables the power exchange monitoring with the low voltage grid. The battery can be charged from the generated PV and wind power, when the load demand is lower than the generation, or directly from the grid, as illustrated in Fig. 1.

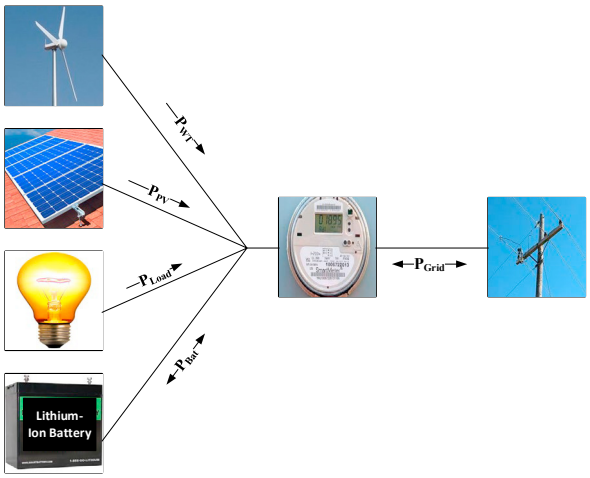

Fig. 1. The architecture of the hybrid energy system

2.1. Solar PV Module Model

The performance model of the solar PV module (SPVM) was developed according to the block diagram presented in Fig. 2 and consists of several blocks. The inputs of the model are the irradiance G, and the ambient temperature T_a, while the output is represented by the SPVM generated power P_{SPV}.

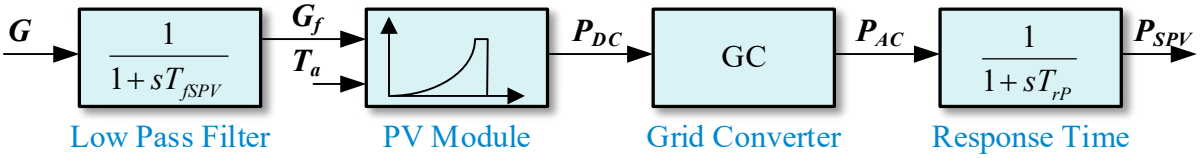

Fig. 2. Block diagram of the SPVM

2.1.1. Low Pass Filter

The solar irradiance G used in this research was collected from a site located in Denmark, with a frequency bandwidth of maximum 5 Hz; thus, the irradiation time series will have a resolution of minimum 200 milliseconds. In order to smoothen the solar irradiance signal, a first order low pass filter was considered. The filtering time constant T_{fSPV} of the SPVM was calculated as presented in [8] according to (1).

$$T_{fSPV} = \frac{1}{2\pi f_{cut-off}} \tag{1}$$

Where the cut-off frequency of the low pass filter is a function of the SPVM power and was determined according to the procedure described in [8].

2.1.2. Low Pass Filter

The output power of an SPVM depends on the ambient temperature T_a and on the solar irradiance G_f (in this case the filtered one) as well as on the performance of the maximum power point tracking (MPPT) algorithm, used to maximize the power conversion between the solar irradiance and the electrical output in the DC link of the power converter P_{DC} [8].

The mathematical model of the SPVM was developed based on (2) – (4) following the methodology presented in [9] and was parameterized based on the parameters of a real PV panel, which are summarized in Table I.

$$I = I_{sc}\left[1 - C_1\left(e^{\frac{V}{C_2 V_{OC}}} - 1\right)\right] \tag{2}$$

$$C_1 = \left(1 - \frac{I_m}{I_{sc}}\right) e^{\frac{V}{C_2 V_{OC}}} \tag{3}$$

$$C_2 = \left(\frac{V_m}{V_{OC}} - 1\right)\left[ln\left(1 - \frac{I_m}{I_{sc}}\right)\right]^{-1} \tag{4}$$

Where, V and I are the voltage and current of the PV module, V_{OC} represents the open circuit voltage, I_{sc} represents the short-circuit current, V_m and I_m represents the MPP voltage and current, respectively.

Table 1. Parameters of the PV module at standard test conditions.

Rated Power	Total Installed Power	No. of PV modules	Vm	Im	VDC	Isc	NOCT	Module Efficiency
360 W	6120 W	17	38.4 V	9.39 A	48.3 V	9.84 A	318 K	18.4 %

2.1.3. Grid Converter

The PV module is connected to the grid converter *GC*, which emulates the power losses of a real PV inverter. Thus, the DC power P_{DC} obtained at the output of the PV module is multiplied by the efficiency of the GC in order to obtain the power fed to the grid. In this work, we have assumed the efficiency of the GC to be 0.985 [8], [10].

2.1.4. Response Time

The response time of the active power injected into the grid is considered in the point-of-connection (PoC). Considering the small scale of the system, the response time T_{rP} is in the same range as the one of the low pass filter.

2.2. Wind Turbine Model

The structure of the performance model of the small wind turbine is presented in Fig. 3. The model has a bandwidth of maximum 1 Hz and is suitable for energy management studies, where only the output power of the WT is required.

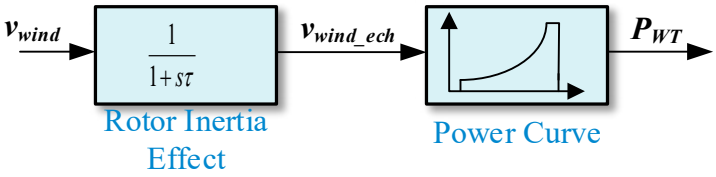

Fig. 3. Block diagram of the wind turbine

2.2.1. Rotor Inertia Effect

The WT's rotor inertia smoothens the time and position variability of the wind speed on the WT's rotor plan [8]. In order to consider this smoothing effect, a first order filter was considered. The time constant τ of the filter was computed based on [8], [11], [12], according to (5).

$$\tau = \tau_0 \frac{v_{rated}}{v} \tag{5}$$

Where, v_{rated} is the rated speed of the wind turbine, v is the actual wind speed and τ_0 is the natural time constant which depends nonlinearly on the WT rated power.

2.2.2. Power Curve

The power curve is a one-dimensional look-up table, which relates the wind speed with the power production of the WT. For this work, a 10 kW small WT was considered, with the main parameters summarized in Table II and the power curve presented in Fig. 4. Furthermore, it has to be highlighted that the WT was certified for the Danish market [13].

Table 2. Parameters of the WT [14]

Rated Power	Cut-in speed	Rated speed	Survival speed	Rotor diameter
10 kW	3 m/s	9 m/s	55 m/s	9.7 m

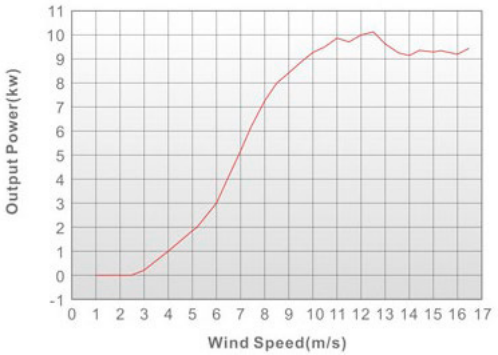

Fig. 4. Power curve of the 10 kW WT [14].

2.3. Lithium-Ion Battery Model

The Li-ion battery performance model is based on a Thevenin equivalent electrical circuit (EEC), as illustrated in Fig. 5. The total requested power $P_{request}$ is divided by the DC link voltage V_{DC} in order to obtain the battery load current I_{bat}. The load current is multiplied by the battery voltage V_{bat}, which is predicted by the EEC, in order to obtain the delivered or absorbed battery power P_{bat}.

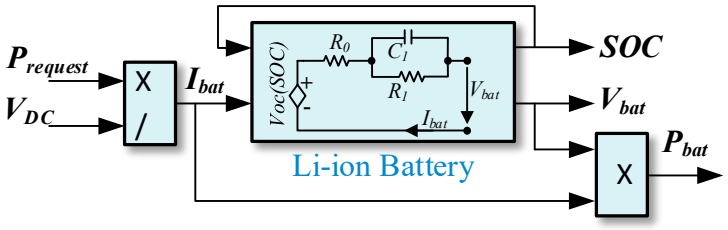

Fig. 5. Block diagram of the lithium-ion battery model.

In order to model the performance behavior of the Li-ion battery, a Thévenin-based EEC was selected as a trade-off solution between estimation accuracy and computation burden [15]. The EEC is composed of a voltage source, which emulates the open circuit voltage of the battery, a series resistance R_0 which represents the battery ohmic resistance and an RC parallel network (R_1 and C_1) used to simulate the charge transfer and diffusion processes inside the battery. Thus, the Li-ion battery voltage is calculated according to (6) and the state-of-charge (SOC) is obtained based on the Coulomb counting approach (7).

$$V_{bat} = V_{OC} \pm V_{EEC} \tag{6}$$

$$OC = SOC_i \pm \frac{1}{C}\int I_{bat}dt \tag{7}$$

Where V_{oc} represents the open circuit voltage of the battery, V_{EEC} represents the voltage drop across the EEC of the battery, SOC_i represents the initial SOC, and C represents the battery capacity

Capacity measurements, open circuit voltage measurements, and internal resistance measurements, using the DC pulse technique, were performed in order to parameterize the Thevenin-based EEC model. As it is well known, the battery performance parameters are very sensitive to the operation conditions [16]. Thus, the charging and discharging capacity of the battery was measured for different current rates (C-rates), the OCV for different SOCs, and the internal resistance at different SOCs and for different charging and discharging C-rates, according to the procedures presented in [17]. All the measurements were performed at 25°C.

The measurements were performed for a lithium iron phosphate (LFP) – based Li-ion battery with the main electrical parameters summarized in Table III.

Table 3. Electrical parameters of the LFP-based Li-ion battery.

Nominal Capacity	Nominal Voltage	Minimum Voltage	Maximum Voltage	Maximum Current
2.5 Ah	3.3 V	2 V	3.6 V	10 A

The measured capacity and OCV for the considered LFP-based battery are presented in Fig. 6 and Fig. 7, respectively. Furthermore, based on the internal resistance measurements, the values of the EEC parameters, R_0, R_1, and C_1 were derived following the procedure presented in [18], [19]. The variation of these parameters with the SOC for a current pulse of 2.5 A applied during both charging and discharging are presented in Fig. 8.

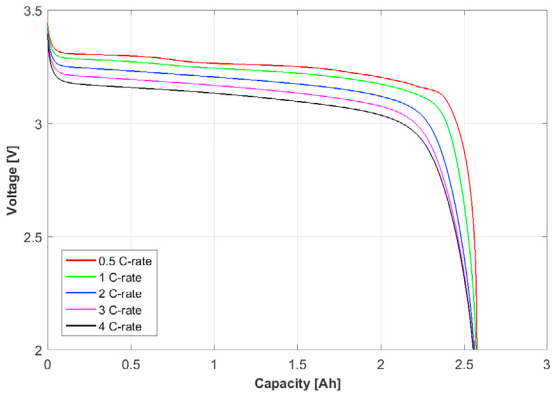

Fig. 6. Dependence of the battery discharging capacity on the C-rate.

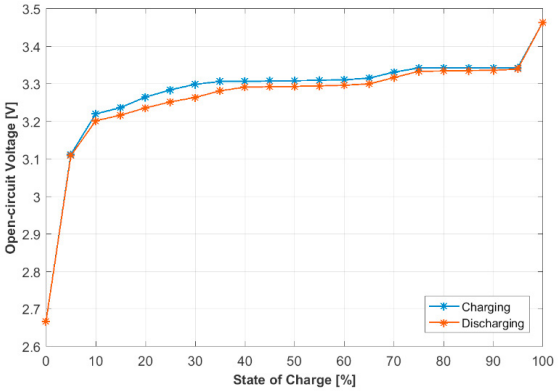

Fig. 7. OCV vs SOC characteristic during charging and discharging.

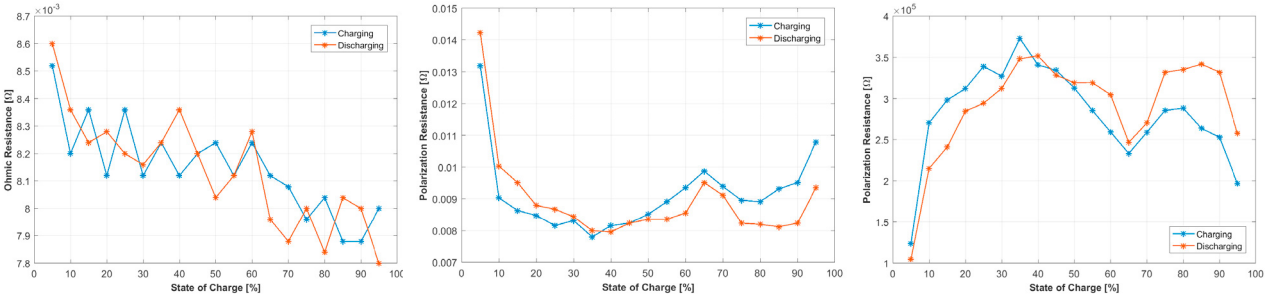

Fig. 8. Variation of the ohmic resistance R_0 (left), resistance R_1 (middle), and capacitance C_1 (left) with the SOC obtained for a 2.5 A (1C-rate) charging and discharging current pulse.

3. Mission Profiles

3.1. Distributed Generation Power Profiles

Real irradiance and wind speed data profiles measured in Denmark, with 5 Hz resolution, were applied to the SPVM and WT models in order to obtain the PV and WT power profiles. For this study, two periods of the year were considered, i.e., one summer day and one winter day. In Fig. 9, the measured irradiance and the corresponding generated PV power profiles are presented, while in Fig. 10, the measured wind speed and the corresponding produced wind power profiles are presented, for both summer and winter day.

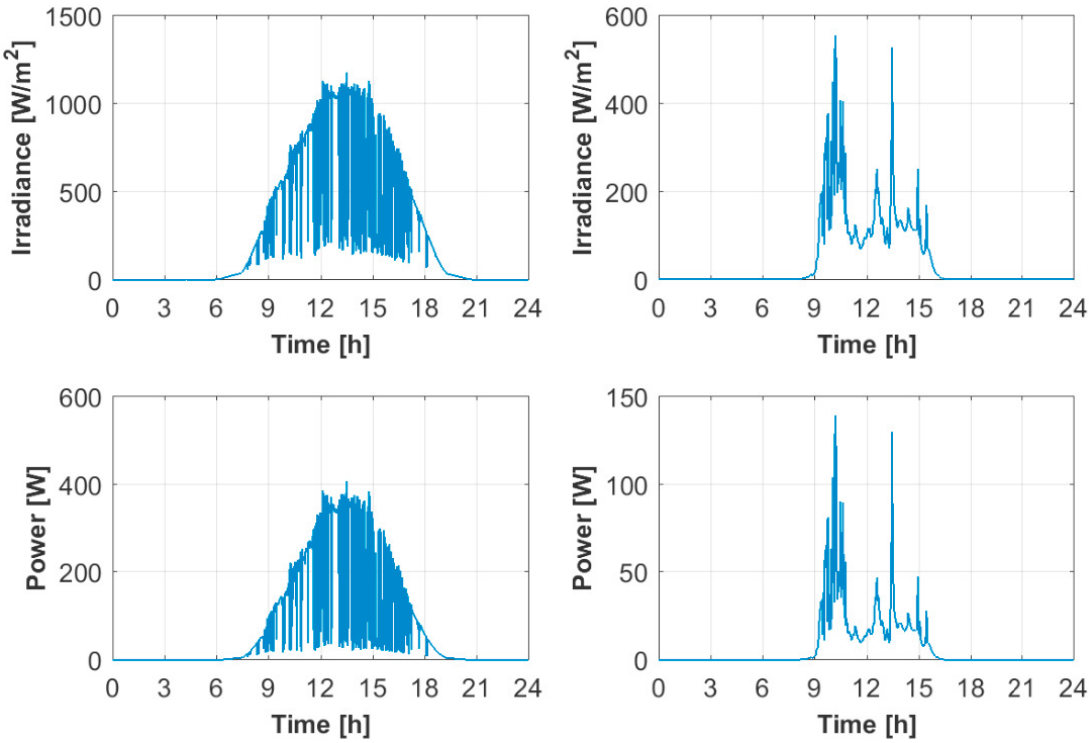

Fig. 9. Irradiance (top) and corresponding PV power (bottom) for one summer day (left) and one winter day (right).

During summer, the PV panels start to produce power earlier in the morning than during winter, and the irradiance level reaches almost 1200 W/m2, and only 550 W/ m2 in the winter. Subsequently, the generated PV power reaches approximately 400 W peak for the maximum irradiance in the summer and only 150 W peak in the winter. As shown in Fig.10, the wind is present almost whole day during the summer and just half of the day in the winter and in both cases reaches values of 10 m/s. Consequently, based on the wind speed profiles and considering its characteristics, summarized in Table II, the WT produces power for half of the day during summer and only for few hours during winter, reaching in both cases 7.5 kW.

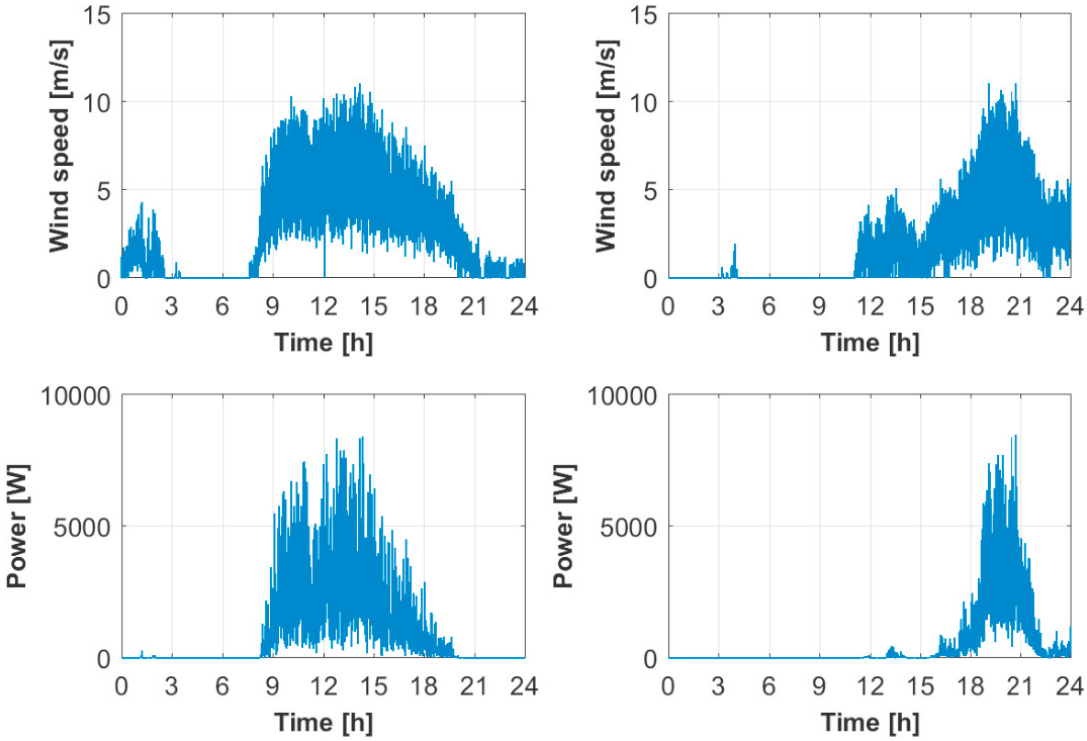

Fig. 10. Wind speed (top) and corresponding WT power (bottom) for one summer (left) and one winter day (right).

3.2. Load Demand Profiles

The load demand profiles used in this work represent the domestic electricity consumption of a residential home in Denmark, according to [20]. Because the household loads and their demands are different depending on the period of the year, one summer and one winter day were considered and the corresponding profiles are presented in Fig. 11.

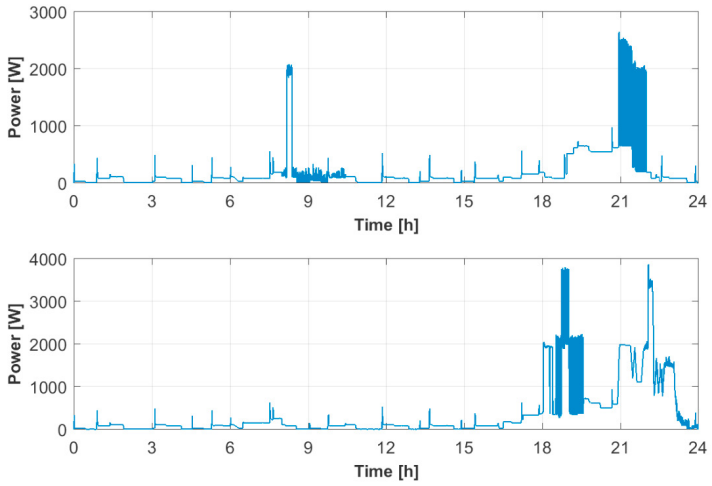

Fig. 11. Residential load demand profile during one summer day (top) and one winter day (bottom).

As it can be observed from Fig. 11, there is a significant difference between the demand during summer and winter; during winter, the higher consumption is generated by the heating and lighting loads, with the power reaching peaks of 4000 W.

4. Results

The performance behavior of the hybrid residential PV – wind system with integrated Li-ion battery storage was investigated for two different energy management strategies, as it will be presented in the next sections.

4.1. Power smoothing

The variable nature of PV and wind power can affect the safe and reliable operation of the low-voltage grid. Thus, before being injected into the utility grid, the power needs to be smoothened. In this work, the proposed solution is the use of a Li-ion battery with a power smoothing algorithm based on a moving average functionality (MAF). The smoothing algorithm calculates a reference power signal P_{out}, by averaging a given series of data for a predefined time interval, which the system will try to track. The power mismatch P_{ref} between the reference power signal obtained from the smoothing algorithm P_{out} and generated power P_{hybrid} represents the reference for the Li-ion battery which charges or discharges accordingly. For this power smoothing application, two cases were considered; the first cases will analyze the system behavior for an averaging time window of 5 minutes, while in the second case the time window is increased to 15 minutes.

4.1.1. Five-minutes moving average

The power injected into the grid after the power smoothing EMS was applied to the hybrid residential system is presented in Fig. 12 for the case of a summer day. The difference between the generated power and the grid injected power is shown in Fig. 13 together with the corresponding one-day battery SOC. By applying a cycle counting algorithm to the obtained SOC profile, we have found out that the battery was subjected to 3.25 full cycles.

The behavior of the considered hybrid residential energy system for a winter day is presented in Fig. 14 and Fig. 15. Due to a less demanding mission profile, the battery was subjected to only 1.4 full cycles.

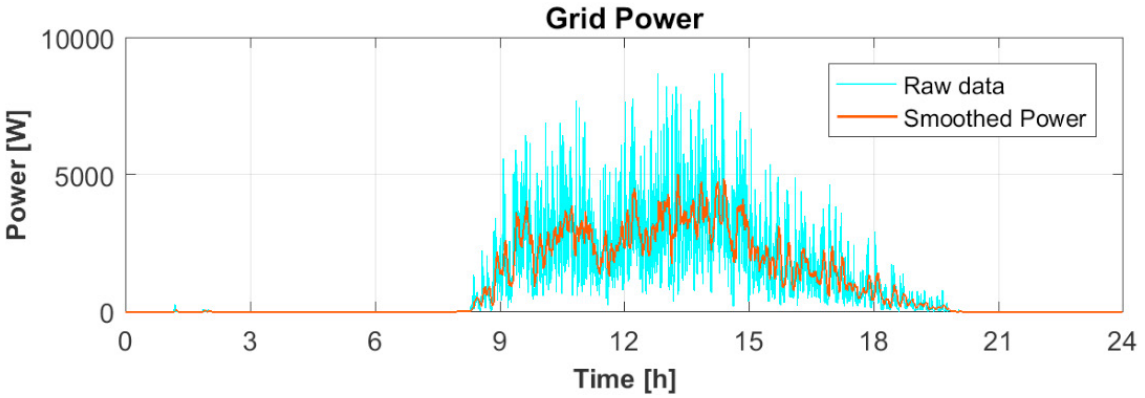

Fig. 12. Comparison between the generated power by the hybrid system and the smoothed grid-injected power – summer.

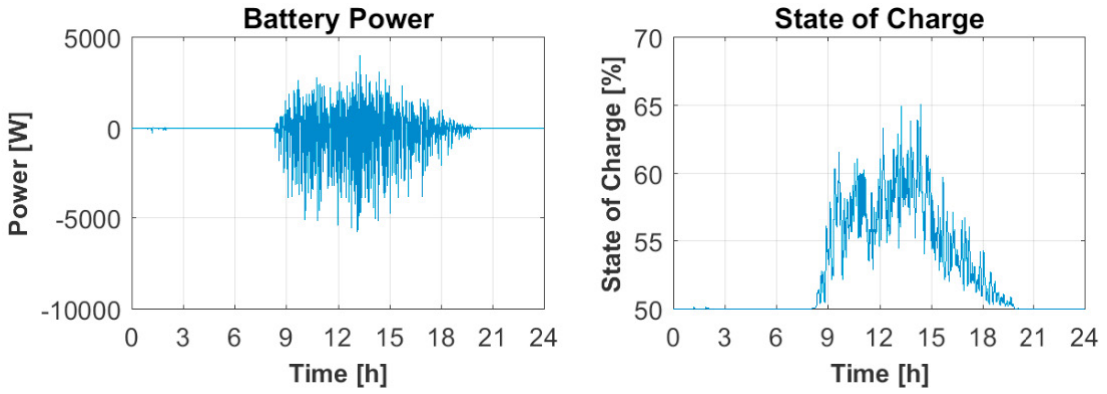

Fig. 13. Battery behavior: power (left) and SOC profile (right) – summer.

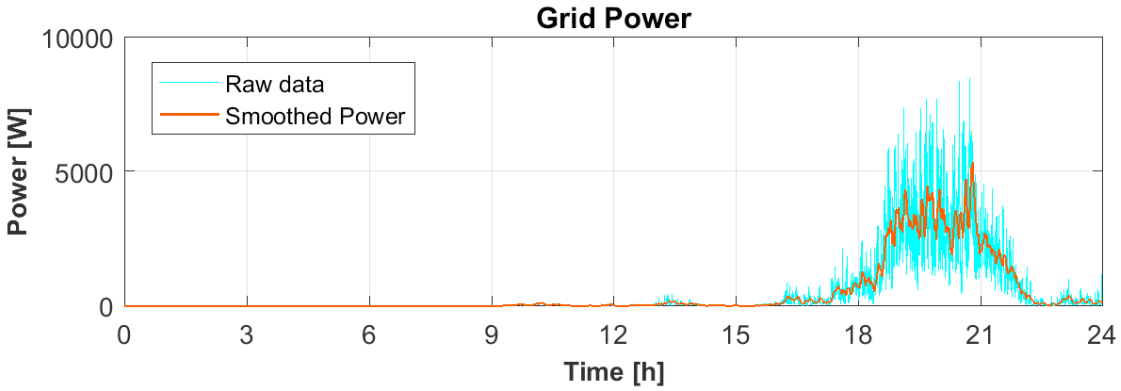

Fig. 14. Comparison between the generated power by the hybrid system and the smoothed grid-injected power – winter.

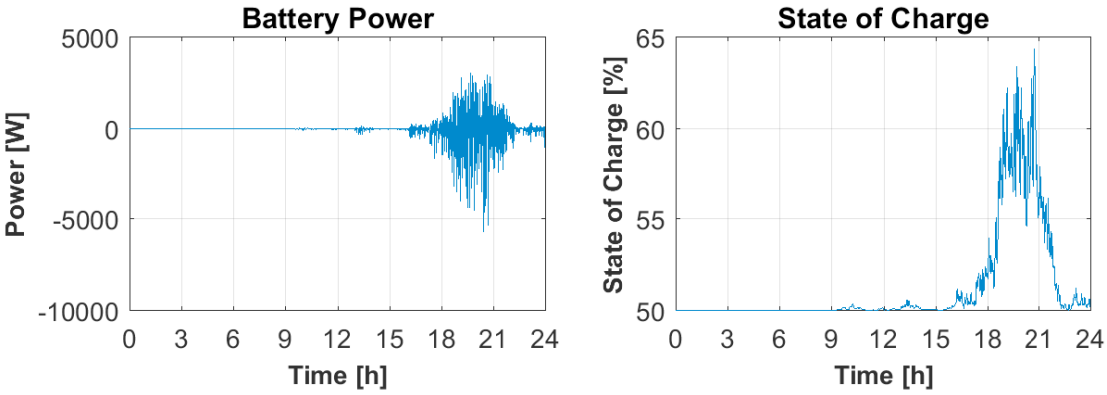

Fig. 15. Battery behavior: power (left) and SOC profile (right) – winter.

4.1.2. Fifteen-minutes moving average

The results obtained for the power smoothing EMS when a 15 minutes moving average filtering algorithm had been used are presented in Fig. 16 – Fig. 19. Because of a greater moving average time window, the power injected into the grid is smoother. On the other hand this has caused bigger battery SOC excursions; however, the number of cycles to which the battery was subjected stayed almost unchanged, i.e., 3.33 and 1.5 cycles for summer and winter cases, respectively.

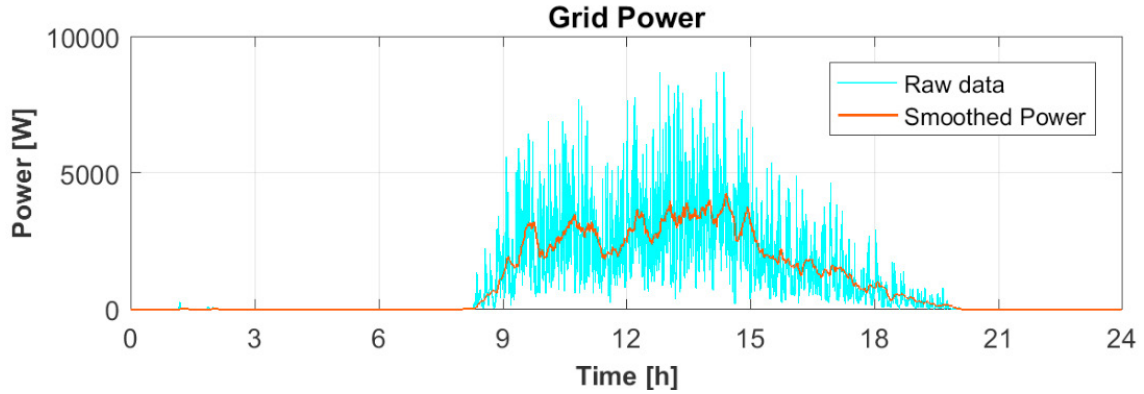

Fig. 16. Comparison between the generated power by the hybrid system and the smoothed grid-injected power – summer.

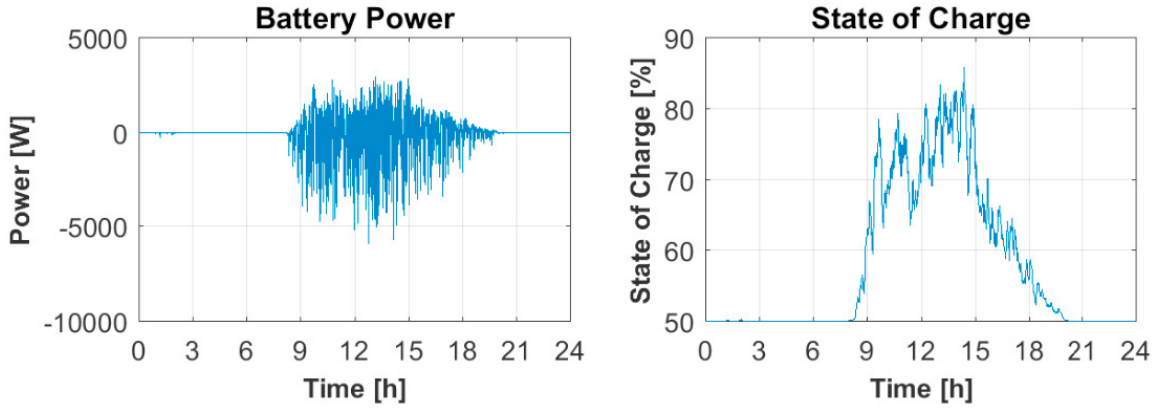

Fig. 17. Battery behavior: power (left) and SOC profile (right) – summer.

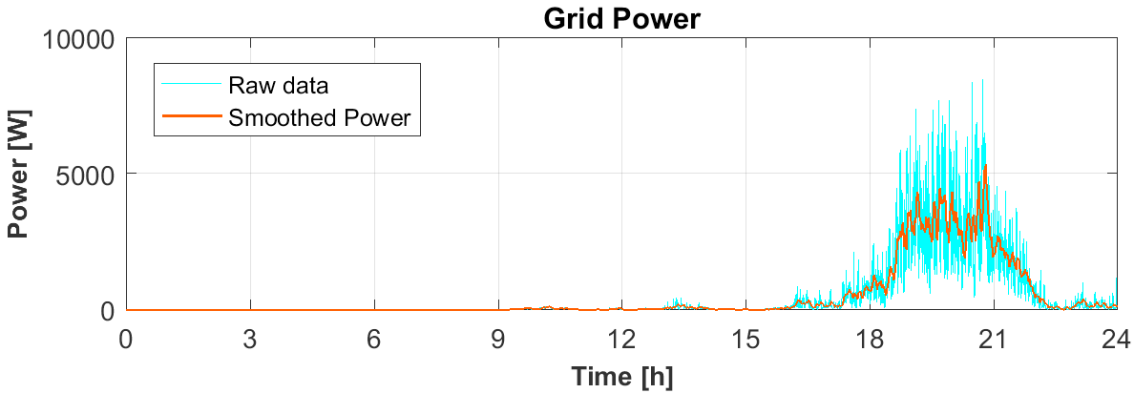

Fig. 18. Comparison between the generated power by the hybrid system and the smoothed grid-injected power – winter.

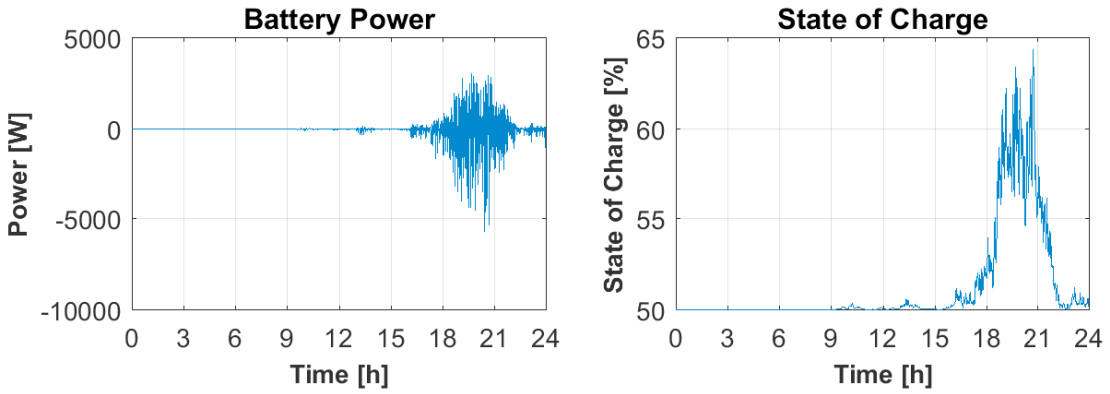

Fig. 19. Battery behavior: power (left) and SOC profile (right) – winter.

4.2. Energy Blocks

Energy storage systems have the flexibility to operate within the electricity market and thus improve the value of the renewable energy. The scope of the energy blocks EMS is to minimize the amount of energy bought from the utility grid and sell a part of the excess production. The proposed scheme is to calculate a 15 minutes power average that will be exchanged with the utility grid. In Fig. 20, there are presented the typical power profiles of the hybrid residential system after the generated power has been extracted from the load power. A positive signal denotes that the power has to be bought from the grid and the negative signal denotes that the power is delivered to the grid.

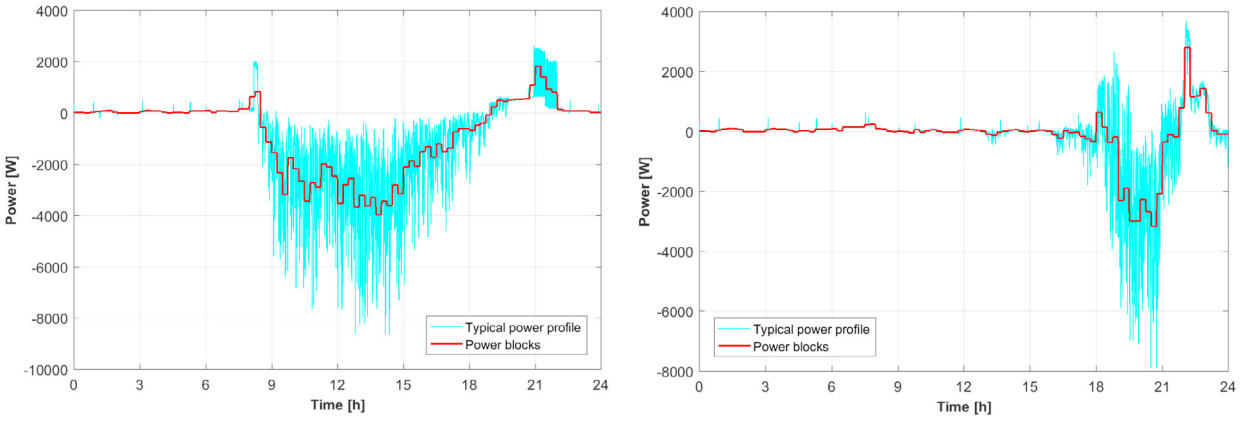

Fig. 20: Typical power profile and power blocks for a summer day (left) and a winter day (right).

The battery power profiles and the corresponding SOC profiles for the two studied cases are presented in Fig. 21 (summer) and Fig. 22 (winter). In both cases, the Li-ion battery is able to provide the energy blocks applications without reaching saturation. Furthermore, similar to the previously studied EMS, the Li-ion battery is stressed more during summer, when it is subjected to 3.67 full cycles, in comparison to winter, when it is subjected to less than half (i.e., 1.75 full cycles).

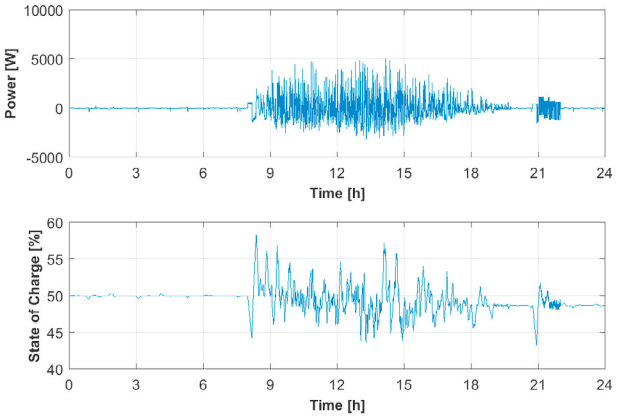

Fig. 21: Battery power and SOC during power blocks EMS for a summer day.

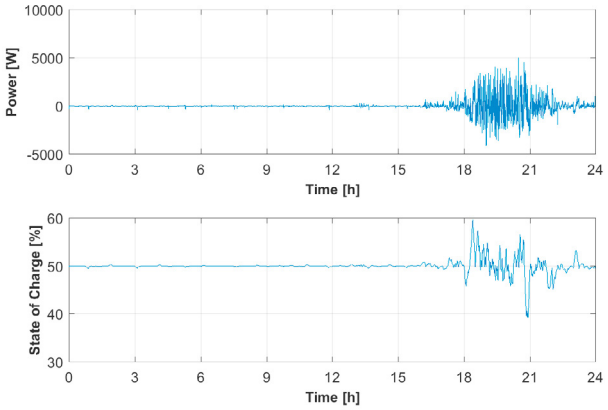

Fig. 22: Battery power and SOC during power blocks EMS for a winter day.

The results summarizing the performance behavior of the considered 6 kW Li-ion battery for the two EMSs are presented in Table IV.

Table 4. Performance behavior of the Li-ion battery for the considered EMSs.

EMS	**Power Smoothing**				**Energy Blocks**	
	5 min. MA		**15 min. MA**			
Period of the year	Summer	Winter	Summer	Winter	Summer	Winter
SOC min [%]	50	50	50	50	43.26	39.18
SOC max [%]	65.11	85.85	64.36	85.83	57.22	59.63
Ah-throughput	16.25	16.66	7.14	7.51	18.35	8.74
FECs	3.25	3.33	1.43	1.50	3.67	1.75

5. Conclusions

In this work, two power and energy management strategies for a hybrid residential PV – wind system with Li-ion battery storage were developed and the behavior of the system was studied. The strategies were focused on the Danish market by using real generation profiles (i.e., irradiation and wind speed) as well as a load profile, which are characteristic for a site in Denmark. In order to achieve this goal, simple but tailored (for such studies), performance models for PV modules, a small wind turbine, and Li-ion batteries were developed and parameterized. The behavior of the hybrid energy system was evaluated for power smoothing and energy blocks applications for two different scenarios (i.e. a summer day and a winter day). For the power smoothing application, a MAF was considered with two averaging time windows of 5 and 15 minutes. In both cases, the desired smoothing effect was achieved, while the battery was subjected to approx. 3.4 and 1.5 full cycles, for a summer and winter day, respectively. Furthermore, the battery was used to maximize the usage of the renewable energy and minimize the electricity bill, by minimizing the energy bought from the utility grid. This was achieved by computing a 15-minutes average power curve for an entire day, by considering the load profile of the house and the produced renewable energy. The difference between the computed curve and the overall house power curve was charged/discharged from the battery. For the considered size of the battery (i.e., 6 kW), the maximum power of the battery was never reached while the Li-ion battery was subjected to 3.75 full cycles during a summer day and 1.75 full cycles during a winter day.

References

[1] IRENA, http://resourceirena.irena.org/gateway/countrySearch/?countryCode=DNK (retrieved 05.02.2018)
[2] Dansk Solcelle Forening, http://solcelleforening.dk/ (retrieved 05.02.2018)
[3] Energistyrelsen, "Danish Energy Agency." https://ens.dk/ (retrieved 05.02.2018)
[4] S. Vazquez, S. Lukic, E. Galvan, L.G. Franquelo, J.M. Carrasco, "Energy Storage Systems for Transport and Grid Applications," *IEEE Transactions on Industrial Electronics*, 57(12) (2010): 3881-3895.
[5] A. Akhil et al., "DOE/EPRI 2013 Electricity Storage Handbook in Collaboration with NRECA," Tech. Rep. SAND2013-5131 (2014).
[6] A.-I. Stan, M. Swierczynski, D.-I. Stroe, R. Teodorescu, S. J. Andreasen, "Lithium Ion Battery Chemistries from Renewable Energy Storage to Automotive and Back-up Power Applications," *2014 International Conference on Optimization of Electrical and Electronic Equipment (OPTIM)*, (2014): 713-720.
[7] B. Zhou et al., "Smart home energy management systems: Concept, configurations, and scheduling strategies," Renewewable Sustainable Energy Reviews 61 (2016): 30–40.
[8] L. Petersen, F. Iov, K. Shahid, R. L. Olsen, M. Altin, A. D. Hansen, "Voltage control support and coordination between ReGen plants in distribution systems," Deliverable D2, November 2016, www.replanproject.dk;
[9] C.-I. Ciontea, D. Sera, and F. Iov, "Influence of Resolution of the Input Data on Distributed Generation Integration Studies". *2014 International Conference on Optimization of Electrical and Electronic Equipment (OPTIM)*, (2014).
[10] ABB, ABB inverter station - PVS800-IS - 1.75 to 2 MW: Product description.
[11] M. Pathmanathan, W.L. Soong and N. Ertugrul C. Tang, Effects of Inertia on Dynamic Performance of Wind Turbines.: *Proceed of Australasian Universities Power Engineering Conference, AUPEC 2008*, (2008): 14-17.
[12] A. Gonzalez Rodriguez and M. Burgos Payan A.G. Gonzalez Rodriguez, "Estimating Wind Turbines Mechanical Constants," *Proceed. of "International Conference On Renewable Energies And Power Quality (Icrepq'07)*, (2007).
[13] "Nordisk Folkecenter for vedvarende energi." http://www.folkecenter.dk/dk/rd/vindkraft/smaa_vindmoller/godkendte-husstandsvindmoeller-i-danmark/. (retrieved 05.02.2018)
[14] Osiris Energy, http://www.osirisenergy.com/ (retrieved 05.02.2018)
[15] R. Jackey et al., "Battery Model Parameter Estimation Using a Layered Technique: An Example Using a Lithium Iron Phosphate Cell", *SAE Technical Paper* (2013).
[16] D.-I. Stroe, M. Swierczynski, A.-I. Stroe, S. K. Kær, "Generalized Characterization Methodology for Performance Modelling of Lithium-Ion Batteries", *Batteries* 2(4) (2016): 37-58.
[17] A.-C. Zaharof, "Power and energy management of a residential hybrid photovoltaic-wind system with battery storage," MSc. Thesis, Aalborg University, June 2017.
[18] A. Hentunen, T. Lehmuspelto, J. Suomela, "Time-Domain Parameter Extraction Method for Thévenin-Equivalent Circuit Battery Models", *IEEE Transactions on Energy Conversion*, 29(3) (2014): 558-566.
[19] A.-I. Stroe et al, "Lithium-ion battery dynamic model for wide range of operating conditions," *Proceedings of 2017 International Conference on Optimization of Electrical and Electronic Equipment (OPTIM) & 2017 Intl Aegean Conference on Electrical Machines and Power Electronics (ACEMP).* (2017): 660-666.
[20] Modelling of household's AC loads, Project report P3 – EN3-305, Aalborg University, (2016).